Nuclear Magnetic Resonance in Antiferromagnetic MnF_2 under Hydrostatic Pressure*

G. B. BENEDEK AND T. KUSHIDA†
Division of Engineering and Applied Physics, Harvard University, Cambridge, Massachusetts
(Received October 23, 1959)

The nuclear magnetic resonance frequency of the F^{19} nucleus in antiferromagnetic MnF_2, in zero external field, has been measured as a function of pressure at 4.2°K, 20.4°K, and 35.7°K using a new type very high frequency variable frequency spectrometer. From these measurements we have deduced the pressure dependence of the hyperfine coupling constant (A) between the manganese electrons and the fluorine nucleus, and the pressure dependence of the Néel temperature. This deduction gives $(1/A)(dA/dP)=+(1.9\pm0.1)\times10^{-6}/(\text{kg/cm}^2)$ and $(1/T_N)(dT_N/dP)=+(4.4\pm0.3)\times10^{-6}/(\text{kg/cm}^2)$. We have also measured the compressibility of MnF_2. The magnitude and pressure dependence of A is explained using the theories of Mukherji and Das, and Marshall and Stuart, which permit a calculation of the dependence of A on the interatomic distances, starting from the Hartree-Fock self-consistent field wave functions for Mn^{2+} and F^- with the Mn^{2+} wave functions properly adjusted to bring it into agreement with neutron scattering form factor measurements. The theory is in very good agreement with the experimental results.

I. INTRODUCTION

MANGANOUS fluoride, MnF_2, is a nearly ionic crystal. On forming the crystal lattice, in first approximation the manganese atoms become doubly ionized, magnetic Mn^{2+} ions with the configuration $^6S_{\frac{5}{2}}$, while the fluorine atoms become singly charged, nonmagnetic F^- ions in the closed shell configuration $^1S_0$. The magnetic moments on the Mn sites are responsible for the paramagnetism of MnF_2 at temperatures above the Néel temperature T_N. Below T_N, the superexchange interaction[1] and anisotropy fields[2] produce an antiferromagnetic ordering of the Mn^{2+} spins.

Figure 1 shows the position of the F^- and Mn^{2+} ions in the tetragonal unit cell as determined[3] by x-ray diffraction. The lengths of the axes of the unit cell in A are[3] $a=4.8734$, $c=3.3099$, and the F^- and Mn^{2+} ions are located, respectively at $\pm(u,u,0)$; $\pm(\frac{1}{2}+u,\frac{1}{2}-u,\frac{1}{2})$ and $(0,0,0)$; $(\frac{1}{2},\frac{1}{2},\frac{1}{2})$ with $u=0.305$. The magnetic ions are located on two interpenetrating sublattices A and B, one of which is formed by the corner ions, the other is formed by the body centered ions. Neutron diffraction studies[4] show that below T_N the spins in sublattice A are aligned antiparallel to those in B, and that the direction of spin alignment is along the c axis. Also these studies determined the degree of spin alignment or the magnetization of a sublattice $M(T)$ as a function of the temperature. There are two nonequivalent fluorine sites a and b. Although every fluorine sees an arrangement of 3 nearest neighbor Mn^{2+} ions at the distances shown in Fig. 2, the plane of the 4 ions rotates 90° around the c axis going from one fluorine site to the other. In the antiferromagnetic region the spin alignment of neighbors is as shown in Fig. 2 for one type fluorine site, and is the reverse for the other fluorine site.

Clearly, the spin alignment of the magnetic ions will produce at the fluorine sites a strong field whose magnitude will be proportional to the sublattice magnetization $M(T)$. In the hope of securing information on $M(T)$, Bloembergen and Poulis[5] searched for the F^{19} nuclear resonance in MnF_2, but were unable to detect it because the spin relaxation time was too short for the equipment they used. Shulman and Jaccarino, however, succeeded in finding this resonance first in the paramagnetic region[6,7] and soon after in the antiferromagnetic region.[8] They confirmed that the field at each fluorine site was proportional to the sublattice magnetization $M(T)$. However, they discovered that the magnitude of this field was much

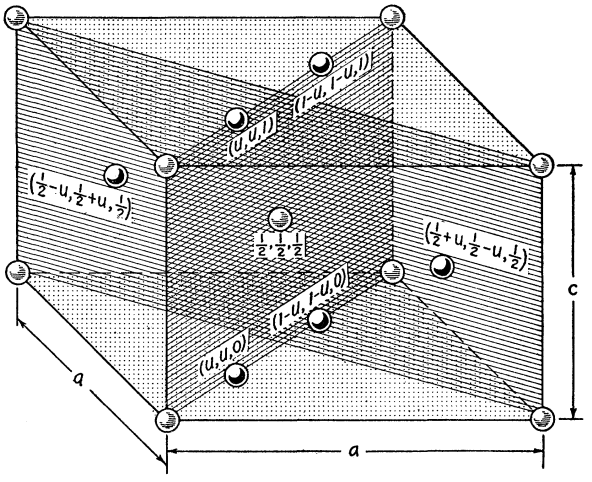

FIG. 1. The unit cell of MnF_2. The black shaded spheres represent the fluorine ions, and the gray shaded ones the manganese ions. $a=4.873$A, $c=3.310$A, and $u=0.305$.

* This research was supported by the office of Naval Research, the Signal Corps of the U. S. Army, and the U. S. Air Force.
† Now at the Department of Physics, Hiroshima University, Hiroshima, Japan.
[1] P. W. Anderson, Phys. Rev. **79**, 350 (1950).
[2] J. A. Eisele and F. Keffer, Phys. Rev. **96**, 929 (1954).
[3] W. H. Baur, Acta Cryst. **11**, 488 (1958).
[4] R. A. Erickson, Phys. Rev. **90**, 779 (1953).
[5] N. Bloembergen and N. J. Poulis, Physica **16**, 915 (1950).
[6] R. G. Shulman and V. Jaccarino, Phys. Rev. **103**, 1126 (1956).
[7] R. G. Shulman and V. Jaccarino, Phys. Rev. **108**, 1219 (1957).
[8] V. Jaccarino and R. G. Shulman, Phys. Rev. **107**, 1196 (1957).

larger than that to be expected from the dipole field of the Mn^{2+} ions. As in the work of Tinkham[9,10] on the electron spin resonance of the manganese ion in ZnF_2, they found[7] that the nondipolar parts of the shifts of the observed F^{19} lines could be accounted for by means of a tensor hyperfine interaction between the time average spin $\langle \mathbf{S}_j \rangle$ of the manganese neighbors, and the nuclear spin I of the fluorine in the form $\mathbf{I} \cdot \sum_j \mathbf{A}_j \cdot \langle \mathbf{S}_j \rangle$. In order to explain the presence of this hyperfine interaction tensor they proposed that the nominally paired spins on the fluorines were slightly unpaired because of an admixture of covalent bonding into the purely ionic configuration.

By studies of the temperature dependence of the F^{19} resonance frequency in the antiferromagnetic region, Jaccarino[11] and Walker were able to obtain extremely accurate measurements of the temperature dependence of the sublattice magnetization $M(T)$. Furthermore, Jaccarino et al. found[12] that below T_N the nuclear resonance could not be observed in precipitated powders of MnF_2. In order to determine if this resulted from a distribution of large internal strains in each of the crystallites Jaccarino et al.[12] subjected a single crystal of MnF_2 to a uniaxial stress and showed that the resonance frequency was indeed a strong function of the stress.

In previous papers we have shown the usefulness of high-pressure measurements in elucidating in detail the electric field gradients in nonconducting crystals,[13] and the hyperfine interaction between the conduction electrons and the nuclei in the alkali metals and copper.[14] High-pressure experiments are a powerful aid to the theory because they provide a means of continually varying the lattice parameters which stand on an equal footing with the temperature in the theoretical description of the state of the solid. Thus, soon after Jaccarino and Shulman's observation of the nuclear resonance in antiferromagnetic MnF_2, the present study was begun in the hope of gaining some insight into the detailed nature of the coupling between the magnetic electrons and the fluorine nuclei. The antiferromagnetic region is especially suitable for these measurements because of the narrowness of the resonance line ($\Delta\nu \sim 50$ kc/sec), compared to the zero field resonance frequency ($\nu \sim 160$ Mc/sec).

From measurements of the pressure dependence of the resonance frequency at 4.2°K, 20.4°K, and 35.7°K, we have deduced the pressure dependence of the Néel temperature T_N, and the hyperfine interaction constant A. By combining this with our measurements of the compressibility of MnF_2, we can determine the dependence of these quantities on the lattice parameters. Finally, we apply the theory of Mukherji and Das,[15] and W. Marshall and R. N. Stuart[16] to the calculation of the magnitude and pressure dependence of the hyperfine interaction constant. This theory represents a new theoretical treatment of the unpairing of spins on the fluorine and enables a straightforward calculation of the degree of this unpairing for all (n,l) groups in the fluorine ion. Agreement of this theory with the experimental results is most satisfactory.

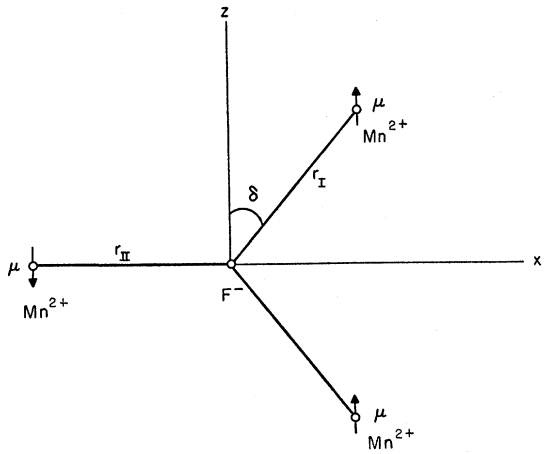

FIG. 2. The arrangement of nearest neighbor Mn^{2+} ions around a fluorine nucleus. The arrows represent the magnitude and relative orientation of the time averaged magnetic moment of the Mn^{2+} ions. A second type fluorine site sees the same configuration as above except that the direction of the Mn spins are reversed.

II. EXPERIMENTAL METHODS AND RESULTS

1. Experimental Methods

The present experiment requires: a sensitive spectrometer capable of reproducing faithfully the line shape of the nuclear resonance in the difficult frequency region around 160 Mc/sec, while the sample is inside a high pressure bomb which is maintained at a rather low temperature ($4.2°K \leqslant T \leqslant 36°K$), a considerable distance (80–90 cm) from the spectrometer. Thus the experimental arrangement consists of three interrelated parts: (1) spectrometer, (2) high-pressure bomb and gas press, and (3) low-temperature system.

By far the most serious experimental difficulty was the vhf spectrometer. When this work was begun, no spectrometer was available which was flexible enough to satisfy our needs. This difficulty was overcome by the invention by one of us (T.K.), of a variable frequency vhf spectrometer, which possesses high sensitivity and good frequency stability. Figure 3 shows this spectrometer. The 6J6 oscillator operates push-pull

[9] M. Tinkham, Proc. Roy. Soc. (London) **A236**, 535 and 549 (1956).
[10] B. Bleaney, Phys. Rev. **104**, 1190 (1956).
[11] V. Jaccarino and L. R. Walker, J. phys. radium **20**, 341 (1959).
[12] J. L. Davis, G. E. Devlin, V. Jaccarino, and A. L. Schawlow, J. Phys. Chem. Solids **10**, 106 (1959).
[13] T. Kushida, G. B. Benedek, and N. Bloembergen, Phys. Rev. **104**, 1364 (1956).
[14] G. B. Benedek and T. Kushida, J. Phys. Chem. Solids **5**, 241 (1958).
[15] A. Mukherji and T. P. Das, Phys. Rev. **111**, 1479 (1958).
[16] W. Marshall and R. N. Stuart (to be published).

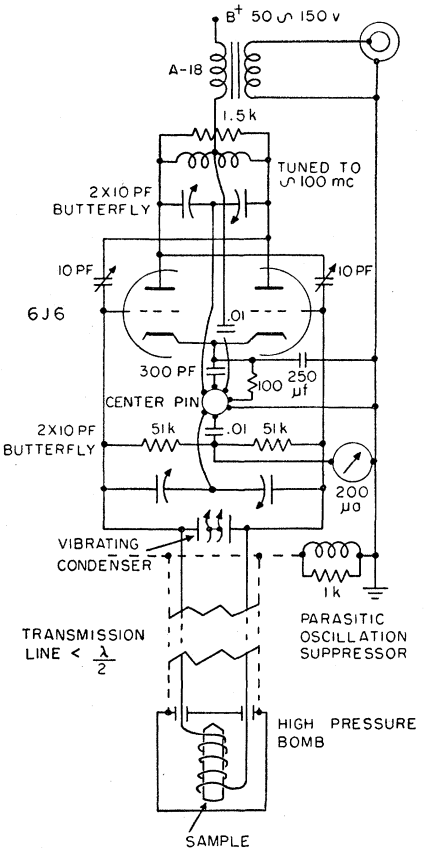

FIG. 3. Circuit diagram of the vhf spectrometer.

as in the lower frequency spectrometer of Volkoff et al.[17] The oscillation frequency is determined by the resonant circuit consisting of the grid butterfly condenser, the sample coil, and the half wavelength transmission line. Initially, without the $\lambda/2$ transmission line, the spectrometer could be operated at 160 Mc/sec only with two small condensers[18] in series with the several turn sample coil. Also the coil had to be very close to the grid circuit. At the suggestion of Bloembergen, a half wavelength Lecher line[19] was inserted between the grid circuit and the sample coil. This proposal succeeded and allowed us to place the sample far from the spectrometer in the low-temperature bath. Furthermore, it was found that by reducing the length of the transmission line by the proper amount from the exact half wavelength value, it was possible to remove entirely the small series condensers. This considerably simplified the problem of resonating the coil inside the high-pressure bomb. A third advantage of the transmission line is that it provides a means of tuning the spectrometer by simply changing the length of the line. This is accomplished by means of telescope-type construction of the transmission line. Tuning by this means is useful since the tuning range of the grid butterfly condenser is limited by the 10–15 $\mu\mu$f stray capacity of the electrical contacts through the high-pressure plug. The overall tuning range of the spectrometer without changing the sample coil was about 15 Mc/sec. Shulman, who is using this spectrometer, has observed that tuning over a much wider range may be achieved by using plug-in inductances at the spectrometer end of the transmission line. The ability to use a several turn sample coil at this frequency is due to the impedance transforming action of the half wavelength transmission line. The effective inductance of the sample coil as viewed at the grid circuit is reduced so much by the transmission line that a 5 turn sample coil may be resonated at $\sim$160 Mc/sec with the grid butterfly condenser. Typical dimensions of the sample coil are: 8 mm i.d. and 11 mm long. The tuning condenser range is 2–10 $\mu\mu$f, while the transmission line is silver plated and 85 cm long.

The oscillation level of the spectrometer may be monitored with the grid current microammeter. This level can be altered by adjusting the capacity of the grid-plate coupling capacitors. Further control of the oscillation level may be obtained by adjusting the plate voltage. In order to obtain very low H_1 values inside the coil the plate voltage may be reduced as low as 50 volts. The rf field inside the coil was measured by observing the saturation of the Br^{81} resonance in $NaBrO_3$, whose relaxation time can be altered by changing the sample temperature. It was found that the minimum value of H_1 obtainable with this spectrometer is about 30 milligauss. This rf field will partially saturate the F^{19} resonance in MnF_2 at 4.2°K; nevertheless, the high sensitivity of the spectrometer produces an almost noise-free F^{19} resonance signal on an oscilloscope screen. It should be mentioned that the grid current meter indicates relative values of the oscillation level only if the plate voltage is kept constant. The microammeter can read the same current for two different plate voltages despite the fact that the rf level does change. An accurate *relative* calibration of the rf level in the coil was obtained using a one turn pickup coil near the sample in conjunction with a crystal diode and galvanometer.

In construction, it is very important to arrange the spectrometer components as symmetrically as possible around both sides of the push-pull circuits to avoid parasitic oscillations. Even with such precautions we have observed that the transmission line permits a parasitic oscillation of frequency much lower than that desired. This parasitic corresponds to an in-phase oscillation of both sides of the push-pull circuits instead of 180° out-of-phase operation. This effect can be eliminated by placing between the shielding sheath of the transmission line and the chassis a strongly Q-damped coil which is roughly resonated with the stray capacity to the parasitic oscillation frequency.

[17] G. Volkoff, H. Petch, and D. Smellie, Can. J. Phys. **30**, 270 (1952).
[18] M. R. Gabillard, Compt. rend. **237**, 705 (1953).
[19] A. Shimauchi, Sci. of Light (Tokyo) **6**, 58 (1957).

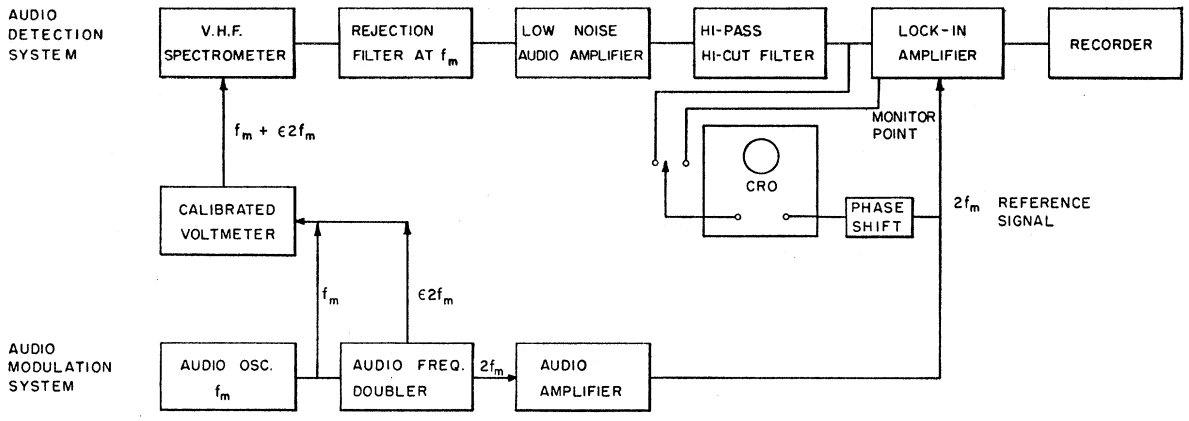

FIG. 4. Block diagram of the audio modulation and detection system.

The modulation and detection scheme is shown in Fig. 4. The frequency of the spectrometer is swept by rotating the shaft of the grid butterfly condenser with a clock motor-gear box arrangement. An audio oscillator at $f_m = 140$ cps drives an audio amplifier which provides the current to drive a vibrating condenser in the spectrometer which modulates the spectrometer frequency at f_m. As the spectrometer frequency passes through resonance the modulation of the nuclear absorption produces a modulation of the oscillation level which appears across the spectrometer plate transformer. It was decided to detect the second derivative of the nuclear absorption line at $2f_m$ because the vibrating condenser inevitably produces considerable amplitude modulation of the rf carrier at f_m. Thus, the audio signal passing out of the spectrometer passes through a very sharp rejection filter at f_m before the low noise audio pre-amplifier and the lock-in which was tuned to $2f_m$. The reference signal for the lock-in is obtained from an audio frequency doubler generating $2f_m$ in phase coherence with the signal at f_m. A small pickup signal at $2f_m$ was found which was produced by second harmonic distortion of the input signal by the vibrating condenser. This small pickup signal was eliminated by introducing a pre-distorted modulation signal into the vibrating condenser. This pre-distorted signal contains components at $2f_m$ whose phase and the amplitude may be adjusted so that output of the spectrometer contains no second harmonic pick up. The output of the lock-in, namely the second derivative of the line is displayed on the recorder. Since we are interested in the position of the line center, this second derivative display was entirely satisfactory. The spectrometer frequency was measured by turning off the modulation and beating the spectrometer against a very stable Gertsch FM-6 heterodyne frequency meter.

The high-pressure beryllium-copper bomb was similar to that previously described[18] except that the pressure transmitting medium, helium gas, was introduced through a plug in one end of the bomb while the rf signal was introduced through a symmetrical two terminal plug on the other end. These plugs were sealed with gold washers in place of the usual lead washers because of the small thermal contraction of gold. The pressure was generated by a gas press consisting of a separator and an intensifier which was kindly loaned to us by Professor W. Paul. The helium gas under pressure was transmitted from the press to the BeCu bomb by means of $\frac{1}{8}$-in. o.d., 0.025-in. i.d. stainless steel high-pressure tubing. The maximum pressure used at each temperature was limited in part by the freezing of helium in the stainless steel tubing. The maximum pressures employed were 100 kg/cm^2 at 4.2°K, 700 kg/cm^2 at 20.4°K, and 1000 kg/cm^2 at 35.7°K.

The low-temperature system, into which the bomb and $\lambda/2$ transmission line extends, is a double Dewar with a glass inner Dewar centered inside a stainless steel outer Dewar. This system maintained a single charge of liquid helium or liquid hydrogen without a change in the bomb temperature over an entire run, a period typically of 6 hours. The run at 35.7°K was carried out with liquid helium as a coolant in the inner Dewar. The height of the bomb above the helium was adjusted till its temperature was near 35.7°K. This temperature was measured using a Leeds and Northrup No. 8164 platinum resistance thermometer placed inside a copper block which was intimately attached to the side of the bomb. The spectrometer frequency was set slightly *below* the resonance frequency at 35.7°K and the bomb temperature was allowed to drift slowly up through the resonance. Thus, temperature sweeping of the line was employed and temperature markers were placed on the recorder chart along with the constant value of the spectrometer frequency. This process was repeated with the spectrometer frequency set slightly *above* the resonance frequency at 35.7°K, and repeated again for a decrease in the bomb temperature which was accomplished by lowering the bomb closer to the helium level. By carrying out this process at each pressure the resonance frequency for any temperature near 35.7°K could be determined as a function of pressure. This somewhat laborious procedure eliminated

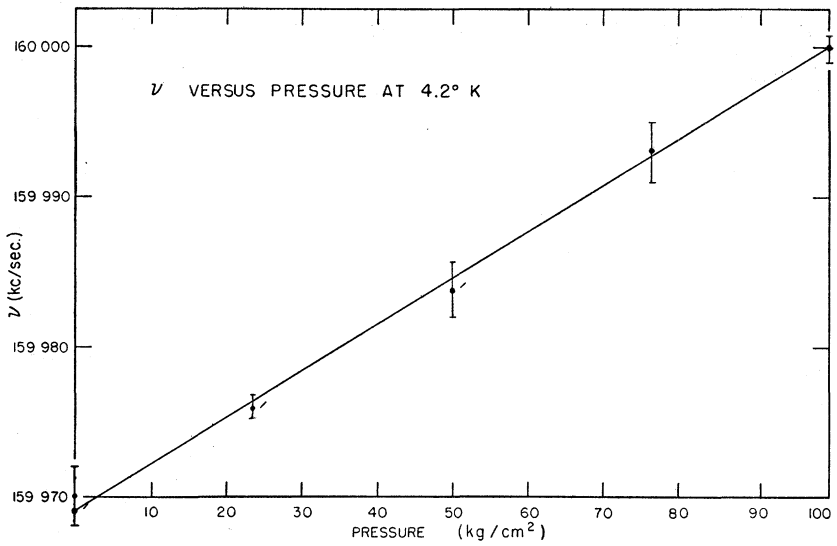

FIG. 5. The pressure dependence of the fluorine resonance frequency in zero external field at 4.2°K.

the need for a complex temperature control for the bomb. Such a system would have had to keep the temperature constant to about 5×10^{-3} °K to eliminate the effects of the strong temperature dependence of ν.

We have also carried out measurements of the fractional change in length of the a and c axes of MnF_2 under hydrostatic pressure by means of the rather crude method of strain gauges glued to the sample. We are aware of the problems of adequate bonding and change in gauge constant under pressure which are inherent in this method. To help eliminate the uncertainties produced by these factors, we measured the change in strain gauge resistance, as the sample was subjected to hydrostatic pressure, simultaneously for the MnF_2 sample and for a sample of pure aluminum whose compressibility is well known. In this way we could determine the compressibility of MnF_2 relative to aluminum, and also determine the gauge constant under hydrostatic pressure. The measurements were repeated twice with two different sets of gauges, and the results, though they showed hysteresis effects, were in large measure consistent. The results presented in the next section represent our estimates for $(1/a)(\partial a/\partial p)$ and $(1/c)(\partial c/\partial p)$ at room temperature along with a conservative estimate of the error involved. Clearly, an independent, more accurate measurement of these quantities using for example an ultrasonic echo method would be most desirable.

2. Experimental Results

Figures 5, 6, and 7 show the F^{19} resonance frequency as a function of pressure at 4.2°K, 20.4°K, and 35.7°K. Over the pressure range studied ν is a linear function of pressure so that we may express these results as shown in the Table I below.

The strain gauge measurements of the compressi-

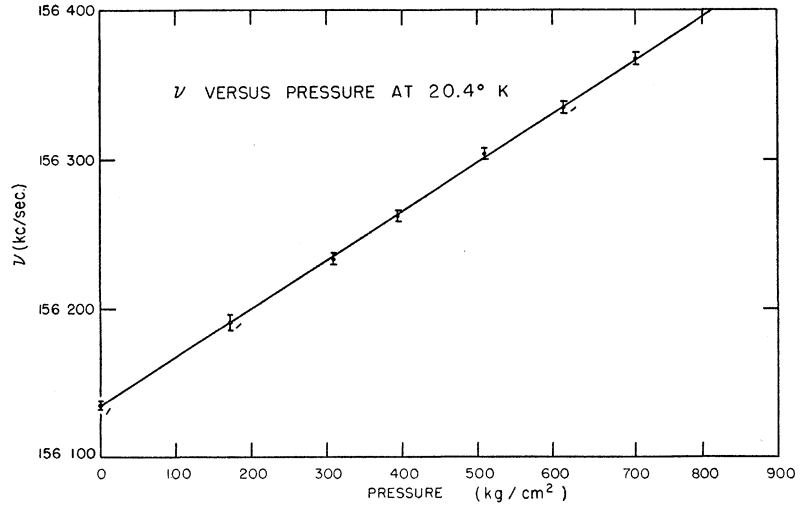

FIG. 6. The pressure dependence of the fluorine resonance frequency in zero external field at 20.4°K.

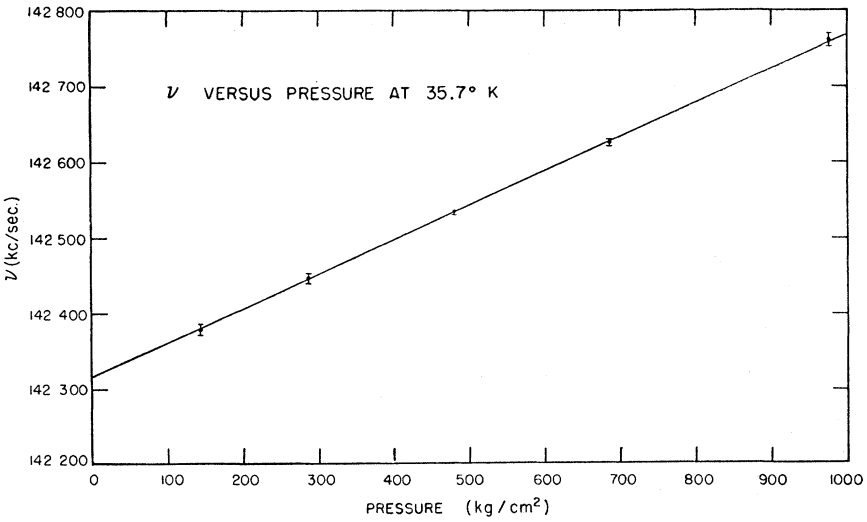

FIG. 7. The pressure dependence of the fluorine resonance frequency in zero external field at 35.7 °K.

bility yield the following for the fractional change in length of the a and c axes:

$$\frac{1}{a}\frac{\partial a}{\partial P}=-(0.45\pm0.03)\times10^{-6}/(\mathrm{kg/cm^2}),$$

$$\frac{1}{c}\frac{\partial c}{\partial P}=-\begin{pmatrix}+0.02\\0.31\\-0.07\end{pmatrix}\times10^{-6}/(\mathrm{kg/cm^2}).$$

III. THEORY

1. Analysis of the Temperature and Pressure Dependence of the Resonance Frequency

The zero field nuclear resonance of the k^{th} fluorine nucleus results from transitions between the energy levels of the Hamiltonian[7]:

$$\mathcal{H}_k=\mathbf{I}_k\cdot\sum_j\mathbf{A}_j\cdot\mathbf{S}_j$$
$$+g_N\beta_N\mathbf{I}_k\cdot\sum_i\left(\frac{3\mathbf{r}_{ik}(\mathbf{r}_{ik}\cdot\mathbf{g}\beta\cdot\mathbf{S}_i)}{r_{ik}^5}-\frac{\mathbf{g}\beta\cdot\mathbf{S}_i}{r_{ik}^3}\right). \quad (1)$$

The first term denotes the hyperfine interaction between the fluorine nuclear spin $\mathbf{I}_k$ and the neighboring manganese electron spins $\mathbf{S}_j$. Since the hyperfine interaction tensor $\mathbf{A}_j$ is a strongly decreasing function of the distance r_{jk}, we carry out the sum j only over the three nearest Mn^{2+} neighbors. The second term represents the dipole-dipole interaction between the fluorine nuclear moment $g_N\beta_N\mathbf{I}_k$ and the electronic magnetic moments $\boldsymbol{\mu}_i=-\beta\mathbf{g}\cdot\mathbf{S}_i$ of all the manganese ions in the lattice. The $\mathbf{g}$ tensor of the manganese is isotropic with $g=2.002$ so that $\beta\mathbf{g}\cdot\mathbf{S}_i=\beta g\mathbf{S}_i$. Furthermore, since the characteristic frequency of spin reorientation of the Mn^{2+} ions is much higher than the nuclear Larmor frequency, we may replace $\mathbf{S}_i$ by $\langle\mathbf{S}_i\rangle$ in computing the energy levels of Eq. (1). The time averaged spin $\langle\mathbf{S}_i\rangle$ in turn is related to the sublattice magnetization $M(T)$ via $\langle\mathbf{S}_i\rangle=-(\frac{5}{2})[M(T)/M_\infty]\hat{n}_i$ where M_∞ is the sublattice magnetization for complete spin alignment or infinite anisotropy field, $\hat{n}_i$ is a unit vector in the direction of M, which, in the antiferromagnetic region, points along the c axis for ions in one sublattice and in the opposite direction for those in the other. From Eq. (1) it follows that the fluorine nuclei in sites a and b see the same magnitude of local field. In passing from the a to the b sites, the direction of the local field, which is parallel to the c axis reverses. Thus the resonance frequency (ν) for nuclei in either site is given by

$$h\nu=(A_{\text{hyp}}+A_{\text{dip}})\tfrac{5}{2}[M(T)/M_\infty], \quad (2)$$

where

$$A_{\text{hyp}}=(2A_{zz}^{\text{I}}-A_{zz}^{\text{II}}), \quad (3)$$

$$A_{\text{dip}}=g_N\beta_N g\beta\sum_i\left(\frac{3\mathbf{r}_{ik}(\mathbf{r}_{ik}\cdot\hat{n}_i)}{r_{ik}^5}-\frac{\hat{n}_i}{r_{ik}^3}\right). \quad (4)$$

In Eq. (4) the sum over neighbor spins should be conducted about the fluorine possessing type I Mn neighbors with magnetic moments pointing up. Lumping together the hyperfine and dipolar interactions we may finally write:

$$h\nu=A\tfrac{5}{2}[M(T)/M_\infty]. \quad (5)$$

TABLE I. The frequency (ν) and pressure dependence ($d\nu/dP$) of the zero field nuclear resonance in antiferromagnetic MnF_2 at three temperatures.

T °K	$\nu(p=0)$ kc/sec	$(\partial\nu/\partial P)$ kc cm²/sec kg
4.2	159 970	0.30 ±0.015
20.4	156 135	0.345±0.006
35.7	142 315	0.457±0.01

a. The Temperature Dependence of ν

The temperature dependence of the resonance frequency arises primarily out of the explicit temperature dependence of the sublattice magnetization $M(T)$. However, ν is a function of temperature also through a possible *explicit* temperature dependence of the interaction constant A, and through the *implicit* temperature dependence of A and $M(T)$ produced by the thermal expansion. Since A can be expected[14] to depend on the temperature through the temperature dependence of the mean-squared amplitude of lattice vibration, we will assume that A is a negligibly weak *explicit* function of the temperature over the temperature range encompassed by our experiments. The *implicit* temperature dependence of ν can be estimated from our data as follows: since $\nu=\nu(a,c,u,T)$, the temperature dependence of ν at constant pressure is given by

$$\left(\frac{\partial\nu}{\partial T}\right)_P=\left(\frac{\partial\nu}{\partial T}\right)_{a,c,u}+\left(\frac{\partial\nu}{\partial a}\right)_{T,c,u}\left(\frac{\partial a}{\partial T}\right)_P+\left(\frac{\partial\nu}{\partial c}\right)_{T,a,u}\left(\frac{\partial c}{\partial T}\right)_P+\left(\frac{\partial\nu}{\partial u}\right)_{T,c,a}\left(\frac{\partial u}{\partial T}\right)_P. \quad (6)$$

Measurements[20] of the thermal expansion coefficients of MnF_2 show that in the temperature range $4°K\leqslant T\leqslant 40°K$, $(\partial a/\partial T)_P$ is negligibly small. We will also neglect $(\partial u/\partial T)$ and write:

$$\left(\frac{\partial\nu}{\partial T}\right)_{a,c,u}\simeq\left(\frac{\partial\nu}{\partial T}\right)_P[1-\delta(T)], \quad (7)$$

where

$$\delta(T)=\frac{c(\partial\nu/\partial c)_{T,a,u}(1/c)(\partial c/\partial T)}{(\partial\nu/\partial T)_P} \quad (8)$$

represents the fractional error involved in neglecting the effect of the thermal expansion. The magnitude of δ may be estimated roughly by setting

$$c\frac{\partial\nu}{\partial c}\sim\frac{\partial\nu}{\partial P}3V\frac{\partial P}{\partial V}. \quad (9)$$

A calculation of δ using our measurements of $(\partial\nu/\partial P)$ and $V(\partial P/\partial V)$ combined with the thermal expansion measurements shows that δ is only of the order of 1% at 20°K and 35.7°K. At 4°K the absence of thermal expansion data is serious, since the magnitude of δ depends in detail on the manner in which $(1/c)(\partial c/\partial T)$ goes to zero because $(\partial\nu/\partial T)$ decreases rapidly as the temperature is lowered. If we assume a relatively slow linear variation of $(\partial c/\partial T)$ with temperature below 10°K, δ is of the order of several percent at 4°K. On the basis of these considerations, we will assume as did Jaccarino,[11] that the temperature dependence of the resonance frequency at constant pressure $(1/\nu)(\partial\nu/\partial T)_P$ is very nearly the same as the explicit temperature dependence of the sublattice magnetization $(\partial\ln M/\partial T)_{a,u,c}$.

b. The Pressure Dependence of ν

The pressure dependence of the resonance frequency comes from pressure produced changes in A and in M. From Eq. (5) we have

$$\frac{1}{\nu}\left(\frac{\partial\nu}{\partial P}\right)_T=\left(\frac{\partial\ln A}{\partial P}\right)_T+\left(\frac{\partial\ln M}{\partial P}\right)_T. \quad (10)$$

In harmony with the discussion above, we will regard $(\partial\ln A/\partial P)_T$ as a constant independent of the temperature T. The pressure dependence of M, $(\partial\ln M/\partial P)_T$, arises out of the dependence of M on the three parameters: (1) M(0), the sublattice magnetization at 0°K; (2) T_A the anisotropy temperature, and (3) T_N the Néel temperature.

The spin wave theory[21] for the antiferromagnetic ground state indicates that $M(0)/M_\infty$ is very close to unity, although estimates range from 0.97 [22] to 0.987.[23] The quantity $M(0)/M_\infty$ is determined primarily by the lattice symmetry and is independent of the size of the unit cell. We shall regard it as independent of the pressure despite the anisotropic compressibility of MnF_2. At 4°K, M is very nearly equal to $M(0)$; thus our assumption that $M(0)/M_\infty$ is independent of pressure immediately leads to the result that $(\partial\ln A/\partial P)=(\partial\ln\nu/\partial P)_{4.2°K}$.

The anisotropy temperature T_A arises primarily out of the dipole-dipole interaction,[24] and can be expected to be an appreciable function of the pressure. However, the magnetization $M(T)$ is a rather weak function of T_A. In fact, if we regard Eisele and Keffer's theoretical expression[2] as a good approximation[25] for $M(T)$, it can be shown at 20°K and 40°K that a reasonable pressure dependence of T_A will produce a negligible pressure dependence of $M(T)$.

Thus, we may regard $M(T)$ as a function of pressure only through T_N. Furthermore, it is consistent with the theory[2] to assume a functional dependence of the general form $M=M(T/T_N)$. From this functional dependence of M on T_N, it follows that one may write

$$\left(\frac{\partial\ln M}{\partial P}\right)_T=-\frac{T}{T_N}\left(\frac{\partial\ln M}{\partial T}\right)_{T_N}\left(\frac{\partial T_N}{\partial P}\right)_T. \quad (11)$$

As shown above, we may replace $(\partial\ln M/\partial T)_{T_N}$ by $(\partial\ln\nu/\partial T)_P$ which is known from Jaccarino's measure-

[20] D. F. Gibbons, Phys. Rev. **115**, 1194 (1959).

[21] P. W. Anderson, Phys. Rev. **86**, 694 (1952).
[22] R. Kubo, Phys. Rev. **87**, 568 (1952).
[23] J. C. Fisher, J. Chem. Phys. Solids **10**, 44 (1959).
[24] F. Keffer, Phys. Rev. **87**, 608 (1952).
[25] F. M. Johnson and A. M. Nethercot, Jr., Phys. Rev. **114**, 705 (1959).

ments.[11,26] We may also regard $(1/T_N)(\partial T_N/\partial P)_T$ as independent of the temperature as we did for $(\partial \ln A/\partial P)$. Hence, we finally find the pressure dependence of ν at temperature T is given by

$$\left(\frac{\partial \ln\nu}{\partial P}\right)_T=\frac{\partial \ln A}{\partial P}-\frac{T}{T_N}\left(\frac{\partial \ln\nu}{\partial T}\right)_P\frac{\partial T_N}{\partial P}. \quad (12)$$

Equation (12) involves only two unknowns: $(\partial \ln A/\partial P)$ and $\partial T_N/\partial P$. Once these are known from measurements of $\partial \ln\nu/\partial P$ at two different temperatures, we can use Eq. (12) to predict $\partial \ln\nu/\partial P$ at a third temperature, thereby enabling a check of the validity of Eq. (12). This was done using the data in Table II with T_N taken[25] as 68°K. Using the data at 4.2°K, $(\partial \ln A/\partial P)$ is given at once as

$$\partial \ln A/\partial P=+(1.9\pm0.1)\times10^{-6}/(\text{kg/cm}^2). \quad (13)$$

Since $(\partial \ln\nu/\partial T)$ is largest at 35.7°K, the data at this temperature was used to determine $(\partial \ln T_N/\partial P)$ giving

$$\partial \ln T_N/\partial P=+(4.4\pm0.3)\times10^{-6}/(\text{kg/cm}^2). \quad (14)$$

From these two results and $(\partial \ln\nu/\partial T)_{20.4°\text{K}}$, Eq. (12) predicts that $(\partial \ln\nu/\partial P)_{20.4°\text{K}}=(2.2\pm0.1)\times10^{-6}/(\text{kg/cm}^2)$. The experimental result is $(\partial \ln\nu/\partial P)_{20.4\text{K}}=(2.21\pm0.04)\times10^{-6}/(\text{kg/cm}^2)$. This satisfactory agreement supports the validity of Eq. (12).

c. *The Magnitude of T_N and A*

In addition to the pressure dependence of A and T_N there is also experimental data on the magnitude of T_N and A.

$$T_N\simeq68°\text{K}. \quad (15)$$

From Eq. (5) we see that $(\frac{5}{2})A$ is equal to the splitting $(h\nu_\infty)$ of the energy levels of the fluorine nucleus in the case of complete spin alignment of each sublattice $(M=M_\infty)$. Complete spin alignment is not attained even at $T=0°\text{K}$, but A can be estimated fairly well from the resonance frequency at 0°K by means of a theoretical estimate for $M(0)/M_\infty$. If we use Fisher's[23] value of $M(0)/M_\infty=0.987$ we find $A=21.63\times10^{-4}$ cm^{-1}. Of course A may be expressed in terms of the physically significant magnetic field (H_∞), which is produced at the fluorine nucleus by complete sublattice spin alignment, i.e.,

$$H_\infty=-\frac{5}{2}\frac{A}{g_N\beta_N}=\frac{h\nu(0)}{[M(0)/M_\infty]g_N\beta_N}. \quad (16)$$

We thus find that

$$H_\infty=40.47\times10^3 \text{ gauss}. \quad (17)$$

Using this with Eq. (13) we find

$$\partial H_\infty/\partial P=(7.7\pm0.4)\times10^{-2} \text{ gauss/(kg/cm}^2). \quad (18)$$

No theoretical explanation for the magnitude and pressure dependence of T_N will be presented here. However, in the following section we shall offer a theoretical calculation of the magnitude and pressure dependence of H_∞.

TABLE II. Experimental data required for the evaluation of $\partial \ln A/\partial P$ and $(\partial T_N/\partial P)$ from Eq. (12).

T °K	$\frac{\partial \ln\nu}{\partial P}\times10^6$ (kg/cm^2)$^{-1}$	$\left(\frac{\partial \ln\nu}{\partial T}\right)_P\times10^3$ (°K)$^{-1}$
4.2	1.9 ±0.1	−0.075±0.15
20.4	2.21±0.04	−3.2 ±0.03
35.7	3.21±0.06	−8.5 ±0.08

TABLE III. The magnitude and pressure dependence of r_I, r_II, and $\lambda\equiv3\cos^2\delta-1$.

r_I in A	2.13	$\partial r_\text{I}/\partial P=-(0.78\ \pm0.1)\times10^{-6}$ A/(kg/cm^2)
r_II in A	2.10	$\partial r_\text{II}/\partial P=-(0.945\pm0.06)\times10^{-6}$ A/(kg/cm^2)
λ	0.812	$\partial\lambda/\partial P=+(0.20\ \pm0.3)\times10^{-6}$/(kg/cm^2)

2. Theoretical Calculation of the Magnitude and Pressure Dependence of H_∞

a. *The Outer Dipole Contribution*

The most obvious contribution to H_∞ comes from the magnetic moments of all the Mn^{2+} ions surrounding a given F nucleus in the lattice. As may be seen from Eq. (4), the three nearest neighbors (n.n.) Mn ions contribute the following:

$$(\mathbf{H}_\infty)_{\text{o.d.}}^{\text{n.n.}}=g\beta\tfrac{5}{2}\left(\frac{2(3\cos^2\delta-1)}{r_\text{I}^3}+\frac{1}{r_\text{II}^3}\right)\hat{n}_z, \quad (19)$$

where r_I, r_II,δ, and the orientation of Mn moments are as shown in Fig. 1.

$$\begin{aligned} r_\text{I}&=[(c/2)^2+2a^2(\tfrac{1}{2}-u)^2]^{\frac{1}{2}},\\ r_\text{II}&=ua\sqrt{2},\\ \cos^2\delta&=(c/2r_\text{I})^2. \end{aligned} \quad (20)$$

Using the x-ray data of Baur for a, c, u, we find for r_I, r_II, and $\lambda\equiv(3\cos^2\delta-1)$ the results listed in Table III. Thus, $(H_\infty)_{\text{o.d.}}^{\text{n.n.}}=12.80\times10^3$ gauss. This result is listed also in Table IV, row 1. Smilowitz[27] has calculated the entire lattice sum [Eq. (4)] and finds $(H_\infty)_{\text{o.d.}}=12.5\times10^3$ gauss. Thus the contribution of farther neighbors is negative and small, amounting to $(H_\infty)_{\text{o.d.}}^{\text{f.n.}}=-0.30\times10^3$ gauss.

We may calculate the pressure dependence of $(H_\infty)_{\text{o.d.}}$ provided that we know the pressure dependence of the bond lengths r_I, r_II. These quantities depend not only on a and c, whose pressure dependence is

[26] V. Jaccarino (private communication).

[27] B. Smilowitz (to be published).

TABLE IV. Numerical values of the various contributions to H_∞ and $(\partial H_\infty/\partial P)$.

in kilogauss		in units of 10^{-2} gauss/(kg/cm^2)	
$(H_\infty)_{\text{o.d.}}^{\text{n.n.}}$	12.80	$(\partial H_\infty/\partial P)_{\text{o.d.}}^{\text{n.n.}}$	1.53 ±0.2
$(H_\infty)_{\text{o.d.}}^{\text{f.n.}}$	−0.30	$(\partial H_\infty/\partial P)_{\text{o.d.}}^{\text{f.n.}}$	−0.036±0.003
$(H_\infty)_{2s}$	24.07	$(\partial H_\infty/\partial P)_{2s}$	6.6 ±2
$(H_\infty)_{1s}$	1.63	$(\partial H_\infty/\partial P)_{1s}$	0.57 ±0.2
$(H_\infty)_{\text{i.d.}}$	1.66	$(\partial H_\infty/\partial P)_{\text{i.d.}}$	0.09 ±0.008
$(H_\infty)_{\text{theor}}$	39.86	$(\partial H_\infty/\partial P)_{\text{theor}}$	8.7 ±2.4
$(H_\infty)_{\text{expt.}}$	40.47	$(\partial H_\infty/\partial P)_{\text{expt.}}$	7.7 ±0.4

known from the compressibility measurements, but also on the internal parameter u whose pressure dependence is not known. Since u varies but little[3] for the homologous rutile structure fluorides, we shall assume that u is a constant independent of the pressure. Under these conditions,

$$\frac{\partial r_{\text{I}}}{\partial P}=\frac{c^2}{4r_{\text{I}}}\left(\frac{1}{c}\frac{\partial c}{\partial P}\right)+\frac{a^2}{2r_{\text{I}}}(1-2u)^2\left(\frac{1}{a}\frac{\partial a}{\partial P}\right), \quad (21)$$

$$\frac{\partial r_{\text{II}}}{\partial P}=r_{\text{II}}\left(\frac{1}{a}\frac{\partial a}{\partial P}\right), \quad (22)$$

and defining $\lambda\equiv(3\cos^2\delta-1)$, we have

$$\frac{\partial\lambda}{\partial P}=6\cos^2\delta\left(\frac{1}{c}\frac{\partial c}{\partial P}-\frac{1}{r_{\text{I}}}\frac{\partial r_{\text{I}}}{\partial P}\right). \quad (23)$$

The numerical results listed in Table III are based on our data of the pressure dependence of a and c. It will be noted that the pressure dependence of $\cos^2\delta$ is so small that it is below the limit of accuracy imposed by the compressibility measurements. We shall therefore take $\partial\lambda/\partial P$ as equal to zero in the numerical calculations which follow. Also, we shall make no attempt to estimate the small changes in $(1/a)(\partial a/\partial P)$ and $(1/c)(\partial c/\partial P)$ produced by lowering the temperature from room temperature to ~4°K.

From Eq. (19) the pressure dependence of $(H_\infty)_{\text{o.d.}}^{\text{n.n.}}$ is given by

$$\left(\frac{\partial H_\infty}{\partial P}\right)_{\text{o.d.}}^{\text{n.n.}}=-\frac{5}{2}\frac{g\beta}{r_{\text{I}}^3}\left[\frac{-6\lambda}{r_{\text{I}}}\frac{\partial r_{\text{I}}}{\partial P}-3\left(\frac{r_{\text{I}}}{r_{\text{II}}}\right)^3\frac{1}{r_{\text{II}}}\frac{\partial r_{\text{II}}}{\partial P}+\frac{2\partial\lambda}{\partial P}\right]. \quad (24)$$

The pressure dependence of the small contribution from farther neighbors may be estimated crudely by taking it as inversely proportional to the volume. Thus:

$$\left(\frac{\partial H_\infty}{\partial P}\right)_{\text{o.d.}}^{\text{f.n.}}=-(H_\infty)_{\text{o.d.}}^{\text{f.n.}}\frac{1}{V}\left(\frac{\partial V}{\partial P}\right). \quad (25)$$

The numerical magnitudes of the o.d. contributions to H_∞ are listed in Table IV.

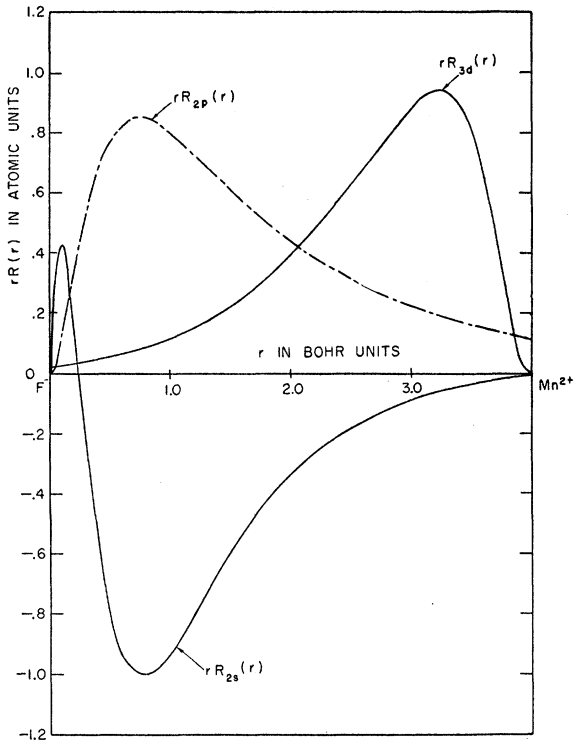

FIG. 8. The normalized radial part of the $3d$, $2s$, and $2p$ Hartree-Fock self-consistent field orbitals for the free Mn^{2+} and F^- ions. The spacing between the Mn^{2+} ion and F^- ion is that found in MnF_2.

b. Isotropic Hyperfine Interaction

As may be seen from Table IV, the outer dipole contribution to H_∞ is but a fraction of the total effect. The remaining contributions to H_∞ come from an unpairing of fluorine spins by the action of the unpaired Mn^{2+} spins. The degree of unpairing of the spins on the fluorine has been calculated theoretically by Marshall and Stuart following the approach of Mukherji and Das. We shall outline the theory of these workers and apply it to the present problem.

Hyperfine interaction with 2s fluorine orbitals. Consider a single $Mn^{2+}-F^-$ pair. Of all the electrons associated with this pair let us deal with those which are situated in the $3d$ orbitals on Mn^{2+}, and also those in the $2s$ and $2p$ orbitals on the fluorine. For the purposes of the present calculation we may regard the $m=0$, $3d$ Mn^{2+} orbital (ϕ_{3d}^0) and the $m=0$, $2p$ F^- orbital (ϕ_{2p}^0) as oriented along the $Mn^{2+}-F^-$ axis. In Fig. 8 is plotted the normalized radial part $[rR(r)]$ of the electronic wave functions for these three orbitals, as given by the Hartree-Fock equation for the *free* ions. It is evident from Fig. 8 that the considerable overlap of the free ion orbitals should alter these orbitals through the effects of Coulomb correlation and exchange. We shall neglect the Coulomb correlation since it is independent of spin and consider physically the effect of the exchange correlation which is required by the Pauli exclusion

principle. The unpairing action of the Pauli principle may be seen most clearly by neglecting, at first, the $2p$ electrons, and considering only the three electrons in the states $\phi_{2s}\alpha$, $\phi_{2s}\beta$, and $\phi_{3d}{}^0\alpha$, where α and β denote the spin states. The $\phi_{2s}\beta$ orbital is unaffected by its overlap with the $\phi_{3d}{}^0\alpha$ orbital because it is orthogonal to it. However, the $\phi_{2s}\alpha$ orbital is not and it will suffer an exchange repulsion with the $\phi_{3d}{}^0\alpha$ orbital. This exchange or Pauli repulsion will act to exclude the α electrons from the region of large overlap and enhance it in the regions of smaller overlap. Thus the probability density for the α spin at the fluorine nucleus will be greater than that of the unaffected β spin, i.e., there will be an "exchange polarization" or unpairing of spins at the fluorine nucleus.

We may treat this problem quantitatively, to first order, by taking as the correct starting wave function the Slater determinant for the three electron system:

$$\Psi(1,2,3)=\frac{1}{[3!(1-|\langle\phi_{2s}|\phi_{3d}{}^0\rangle|^2)]^{\frac{1}{2}}}\times\begin{vmatrix}\phi_{3d}(1)\alpha & \phi_{3d}(2)\alpha & \phi_{3d}(3)\alpha\\ \phi_{2s}(1)\alpha & \phi_{2s}(2)\alpha & \phi_{2s}(3)\alpha\\ \phi_{2s}(1)\beta & \phi_{2s}(2)\beta & \phi_{2s}(3)\beta\end{vmatrix}. \quad (26)$$

The coefficient of the determinant insures the normalization of $\Psi(1,2,3)$. The ϕ's are assumed normalized. The hyperfine interaction between these three electrons and the fluorine nucleus is given by:

$$\mathcal{H}_{\rm hyp}=-g_N\beta_N\mathbf{I}_F\cdot\left(\frac{8\pi}{3}g\beta\sum_{i=1}^{3}\mathbf{S}_i\delta(r_i-r_F)\right)=-g_N\beta_N\mathbf{I}_F\cdot(\mathbf{H}_\infty)_{2s}, \quad (27)$$

where $\mathbf{S}_i$ is the spin of the $i^{\rm th}$ electron ($i=1, 2, 3$). $\mathbf{I}_F$ is the spin of the fluorine nucleus and r_F is the position of the fluorine nucleus. We may determine the field produced by the hyperfine interaction in the first order of perturbation theory by calculating the expectation value:

$$(H_\infty)_{2s}{}^{\rm I}=\left\langle\Psi^*\left|\frac{8\pi}{3}g\beta\sum_{i=1}^{3}S_i\delta(r_i-r_F)\right|\Psi\right\rangle. \quad (28)$$

Evaluating (28) we find

$$(H_\infty)_{2s}{}^{\rm I}=\frac{4\pi}{3}g\beta\frac{|\phi_{2s}(r_F)|^2|\langle\phi_{2s}|\phi_{3d}{}^0\rangle|^2+|\phi_{3d}(r_F)|^2-2\phi_{3d}{}^0(r_F)\phi_{2s}(r_F)\langle\phi_{2s}|\phi_{3d}{}^0\rangle}{1-|\langle\phi_{2s}|\phi_{3d}{}^0\rangle|^2}. \quad (29)$$

By the superscript I we denote the contribution to H_∞ from a single Mn located at a distance $r_{\rm I}$ from the fluorine. $|\langle\phi_{2s}|\phi_{3d}{}^0\rangle|^2$ is the square of the overlap integral between the $2s$ and $3d$ orbitals. The ϕ's are chosen to be real. Equation (29) is the result of Mukherji and Das.[15] Of the three terms in the numerator the $|\phi_{3d}{}^0|^2$ term is negligibly small compared to the first and third terms. These two terms represent the unpairing produced by the exchange correlation. If f_{2s} represents the degree of unpairing we have on factoring $|\phi_{2s}(r_F)|^2$ from Eq. (29) that

$$f_{2s}=\frac{|\langle\phi_{2s}|\phi_{3d}\rangle|^2-2\langle\phi_{2s}|\phi_{3d}\rangle\phi_{3d}{}^0(r_F)/[\phi_{2s}(r_F)]}{1-|\langle\phi_{2s}|\phi_{3d}{}^0\rangle|^2}. \quad (30)$$

It should be noted that in this first-order treatment it is not necessary to calculate the change in the orbitals (ϕ) produced by the exchange repulsion. To do this one could set up the Hartree-Fock equations for each orbital using the free ion ϕ's to determine the different exchange potentials for each equation.[28–31] Using the new ϕ's thereby determined, the hyperfine interaction can be calculated to the second order.

Mukherji and Das evaluated f_{2s} using the most recent[32,33] Hartree-Fock solutions for ϕ_{2s} and $\phi_{3d}{}^0$. However, their result was only half as big as is required to explain Tinkham's observations[9] of the hyperfine structure of the paramagnetic resonance spectrum of Mn^{2+} in ZnF_2. W. Marshall noted, however, that recent neutron diffraction form factor measurements[34] in a number of Mn salts, as well as Erickson's[4] older data on the Mn^{2+} ion in MnF_2, show that the $3d$ orbital is spread out radially by a scaling factor of 1.10 compared with the free ion solution. This produces a much larger $3d-2s$ overlap. The spreading out of the $3d$ orbital may be due to the very considerable overlap of the $2p$ fluorine orbital on the Mn nucleus as shown in Fig. 8. This acts to screen the Mn nucleus from its own electrons. Using the scaling factor obtained from the neutron diffraction data, Marshall and Stuart[16] recalculated the overlap integrals as a function of the Mn–F distance (r) and found the results given in Table V. These results are

TABLE V. The square of the overlap integral $|\langle\phi_{2s}|\phi_{3d}{}^0\rangle|^2$ and the degree of unpairing (f_{2s}) of the $2s$ fluorine orbital as a function of the Mn–F distance.[a]

r in A	$\lvert\langle\phi_{2s}\rvert\phi_{3d}{}^0\rangle\rvert^2$	f_{2s}
2.10	0.491×10^{-2}	0.540×10^{-2}
2.11	0.471×10^{-2}	0.519×10^{-2}
2.12	0.456×10^{-2}	0.502×10^{-2}
2.13	0.440×10^{-2}	0.4828×10^{-2}
2.14	0.423×10^{-2}	0.464×10^{-2}

[a] See reference 16.

[28] J. C. Slater, Phys. Rev. **82**, 538 (1951).
[29] V. Heine, Phys. Rev. **107**, 1002 (1957).
[30] J. H. Wood and G. Pratt, Jr., Phys. Rev. **107**, 995 (1957).
[31] M. H. Cohen, D. A. Goodings, and V. Heine, Proc. Phys. Soc. (London) **73**, 811 (1959).
[32] D. R. Hartree, *Calculation of Atomic Structures* (John Wiley and Sons, Inc., New York, 1957), p. 173.
[33] C. Froese, Proc. Cambridge Phil. Soc. **53**, 206 (1957).
[34] J. M. Hastings, N. Elliott, and L. M. Corliss, Phys. Rev. **115**, 13 (1959).

TABLE VI. The square of the overlap integral $|\langle\phi_{1s}|\phi_{3d}{}^0\rangle|^2$ and the degree of unpairing f_{1s} of the 1s fluorine orbital as a function of the Mn—F distance.[a]

r in A	$\lvert\langle\phi_{1s}\rvert\phi_{3d}{}^0\rangle\rvert^2$	f_{1s}
2.10	0.277×10^{-4}	0.198×10^{-4}
2.11	0.263×10^{-4}	0.189×10^{-4}
2.12	0.251×10^{-4}	0.180×10^{-4}
2.13	0.240×10^{-4}	0.1725×10^{-4}
2.14	0.230×10^{-4}	0.165×10^{-4}

[a] See reference 16.

about double those of Mukherji and Das. It should be observed that f_{2s} differs from $|\langle\phi_{2s}|\phi_{3d}{}^0\rangle|^2$ by the cross term in Eq. (30). This cross term was calculated using the shielded Hartree-Fock solution at the fluorine nucleus. Since $\phi_{3d}(r_F)$ may be considerably altered from this value by the fluorine nucleus, the present calculation of the cross term may not be accurate.

Equation (29) gives the contribution to $(H_\infty)_{2s}$ from a single Mn^{2+} neighbor. To get the effect of the three neighbors we may sum the effects of each neighbor independently and find:

$$(H_\infty)_{2s}=(4\pi/3)g\beta|\phi_{2s}(r_F)|^2(2f_{2s}{}^{\mathrm{I}}-f_{2s}{}^{\mathrm{II}}), \quad (31)$$

where f^{I} and f^{II} are the fractional unpairings due to the neighbors at r_{I} and r_{II}, respectively. This may also be written in the "A" notation of Tinkham[9] or Clogston.[35]

$$H_\infty=(S/g_N\beta_N)(2A_{2s}{}^{\mathrm{I}}-A_{2s}{}^{\mathrm{II}}), \quad (32)$$

where

$$A_{2s}{}^{\mathrm{I,II}}=(g_N\beta_N/S)(4\pi/3)g\beta|\phi_{2s}(r_F)|^2f_{2s}{}^{\mathrm{I,II}}.$$

S is the spin of the Mn^{2+} ion, $\frac{5}{2}$.

Using the results listed in Table V for f_{2s} for the bond lengths r_{I} and r_{II}, and $|\phi_{2s}(0)|^2=10.79$ in Bohr units, we get the values listed in Table IV for $(H_\infty)_{2s}$.

The pressure dependence of $(H_\infty)_{2s}$ is given by

$$\left(\frac{\partial H_\infty}{\partial P}\right)_{2s}=\frac{4\pi}{3}g\beta|\phi_{2s}(r_F)|^2 \times\left(2\frac{\partial f_{2s}{}^{\mathrm{I}}}{\partial r_{\mathrm{I}}}\frac{\partial r_{\mathrm{I}}}{\partial P}-\frac{\partial f_{2s}{}^{\mathrm{II}}}{\partial r_{\mathrm{II}}}\frac{\partial r_{\mathrm{II}}}{\partial P}\right). \quad (33)$$

The numerical value of this contribution to the pressure dependence of H_∞ is listed in row 3, of Table IV. It should be noted that the large uncertainty listed for this number comes from the uncertainty in the measurement of the compressibility.

We may also calculate the contribution to H_∞ from the unpairing of the 1s electrons in exactly the same way as has been outlined above for the 2s electrons. The overlap integrals and the fractional unpairings f_{1s} are listed in Table VI as a function of the Mn—F distance. Using these and $|\phi_{1s}(r_F)|^2=19.6|\phi_{2s}(r_F)|^2$, we find the results on row 4 of Table IV.

c. The Anistropic Hyperfine Interaction

The overlap of the 2p fluorine orbitals with the 3d orbital of the manganese produces an unpairing of the spins in the 2p states. These unpaired spins produce an additional "inner dipole" contribution to the magnetic field at the fluorine nucleus. To determine this field, consider first the effect of a single Mn neighbor. Let the three 2p orbitals be denoted by p_σ, $p_{\pi'}$, p_π where these orbitals point respectively along the bond, along the y direction and along the third mutually perpendicular direction. Also, let $f_{p\sigma}$, $f_{p\pi'}$, $f_{p\pi}$ be the fractional unpairing of the spins in each of these orbitals produced by the overlaps with the 3d orbitals. The direction of the unpaired spin in each orbital is of course the same as that of the Mn^{2+} neighbor. The contribution to the inner dipole field can then be calculated for these three orbitals in a straightforward manner. The net effect of the three nearest neighbor Mn^{2+}'s can be obtained by adding together the contribution of each neighbor independently. If the superscripts I, II refer to type I, and type II Mn neighbors we find that the inner dipole field is

$$(H_\infty)_{\mathrm{i.d.}}=\frac{2(3\cos^2\delta-1)A_\sigma{}^{\mathrm{I}}-2A_\pi{}^{\mathrm{I}}+A_\sigma{}^{\mathrm{II}}+A_\pi{}^{\mathrm{II}}}{(g_N\beta_N/S)}. \quad (34)$$

where $S=\frac{5}{2}$, and where

$$A_\sigma{}^{\mathrm{I,II}}=\frac{2}{5}\left\langle\frac{1}{r^3}\right\rangle\frac{g_N\beta_N}{S}\frac{g\beta}{2}(f_{p\sigma}{}^{\mathrm{I,II}}-f_{p\pi'}{}^{\mathrm{I,II}}), \quad (35)$$

$$A_\pi{}^{\mathrm{I,II}}=\frac{2}{5}\left\langle\frac{1}{r^3}\right\rangle\frac{g_N\beta_N}{S}\frac{g\beta}{2}(f_{p\pi}{}^{\mathrm{I,II}}-f_{p\pi'}{}^{\mathrm{I,II}}). \quad (36)$$

The quantity

$$\left\langle\frac{1}{r^3}\right\rangle=\int_0^\infty\frac{r^2dr|R_{2p}(r)|^2}{r^3}$$

is the average value of $1/r^3$ taken over the radial part of the 2p orbital. The squares of the overlap integrals $f_{p\sigma}=|\langle\phi_{2p}{}^0|\phi_{3d}{}^0\rangle|^2$ and $f_{p\pi'}=|\langle p_x|d_{zx}\rangle|^2$ are listed in Table VII as a function of the distance r. The quantities

TABLE VII. The squares of the overlap integrals $f_{p\sigma}$ and $f_{p\pi'}$ between the p orbitals on the fluorine and the d orbitals on the manganese ion as a function of the Mn—F distance.[a]

r in A	$f_{p\sigma}$	$f_{p\pi'}$
2.10	0.675×10^{-2}	0.281×10^{-2}
2.11	0.663×10^{-2}	0.272×10^{-2}
2.12	0.651×10^{-2}	0.263×10^{-2}
2.13	0.640×10^{-2}	0.254×10^{-2}
2.14	0.629×10^{-2}	0.245×10^{-2}

[a] See reference 16.

[35] A. M. Clogston (private communication).

A_π^{I} and A_π^{II} are zero because $f_{p\pi}=f_{p\pi'}$. It should be noted that in Eqs. (34), (35), and (36) we have assumed that the degree of unpairing in the p orbitals is uniform throughout each orbital. This is not, in fact, the case since the cross term shown in Eq. (30) is a function of the distance between the Mn ion and the point in the p orbital at which the unpairing is to be calculated. We are therefore neglecting entirely the effect of the cross term in assuming the unpairing to be uniform and equal to the square of the overlap integral. This procedure probably introduces little error in the calculation of H_∞ and dH_∞/dP because the inner dipole contribution to these quantities is in itself quite small. Using[36] $\langle 1/r^3\rangle=44.4\times10^{24}/\mathrm{cm}^3$, we find the value of $(H_\infty)_{\mathrm{i.d.}}$ listed in Table IV.

The pressure dependence of $(H_\infty)_{\mathrm{i.d.}}$ is given by

$$\left(\frac{\partial H_\infty}{\partial P}\right)_{\mathrm{i.d.}}=\frac{2}{5}\left\langle\frac{1}{r^3}\right\rangle\frac{g\beta}{2}\left(2\lambda\frac{\partial(f_{p\sigma}^{\mathrm{I}}-f_{p\pi'}^{\mathrm{I}})}{\partial r_{\mathrm{I}}}\frac{\partial r_{\mathrm{I}}}{\partial P}+\frac{\partial(f_{p\sigma}^{\mathrm{II}}-f_{p\pi'}^{\mathrm{II}})}{\partial r_{\mathrm{II}}}\frac{\partial r_{\mathrm{II}}}{\partial P}+2(f_{p\sigma}^{\mathrm{I}}-f_{p\pi'}^{\mathrm{I}})\frac{\partial\lambda}{\partial P}\right). \quad (37)$$

The magnitude of this term is listed in Table IV.

It is clear from the last two rows of Table IV that the theoretical calculations of H_∞ and dH_∞/dP are in excellent agreement with the experimental results.

It may be worthwhile to emphasize that the theory outlined above does not require the inclusion of any covalency, in that we do not include the unpairing effect of fluorine electrons "hopping" into d states on the manganese ion. Clearly our results indicate that this is well justified at least in connection with the s-state electrons. "Hopping" out of p orbitals may affect the f_p's somewhat, however, as has been noted above, the error thereby produced in the calculation of H_∞ and dH_∞/dP will be quite small due to the small contribution of the inner dipole field.

[36] R. G. Barnes and W. V. Smith, Phys. Rev. **93**, 95 (1954).

IV. CONCLUSIONS

From our measurements of the pressure dependence of the zero field nuclear magnetic resonance frequency of the F^{19} nucleus in antiferromagnetic MnF_2, we have deduced the pressure dependence of the Néel temperature, and the pressure dependence of the hyperfine interaction between the fluorine nucleus and the manganese electrons. No theoretical explanation is offered for the pressure dependence of T_N.

The theories of Mukherji and Das, and Marshall and Stuart are used to explain the magnitude and pressure dependence of the hyperfine interaction. The theory uses the Hartree self-consistent field wave functions for free fluorine ions, with the Hartree solution for the Mn^{2+} ion slightly altered to bring it into agreement with neutron scattering form factor measurements. The electron unpairing responsible for the hyperfine interaction is calculated solely from the effects of exchange correlation which arise directly out of the Pauli Exclusion Principle. Agreement between theory and experiment is very good.

V. ACKNOWLEDGMENTS

The authors acknowledge, with thanks, discussions of the theory of the hyperfine interaction with Dr. Walter Marshall, who generously made his calculations with R. N. Stuart available to us before publication. We are also grateful to Dr. V. Jaccarino for the transmission of data prior to publication. The single crystal samples used were provided by Dr. V. Jaccarino, Dr. J. W. Nielson of the Bell Telephone Laboratories, Dr. S. Foner of Lincoln Laboratory, and Dr. J. W. Stout of the University of Chicago. The x-ray orientation of the single crystal used for the compressibility measurement was kindly made by Dr. N. Kato. Professor W. Paul helped us through the loan of a high-pressure gas press.